AJNR Am J Neuroradiol 20:1349–1357, August 1999

Relationship between MR Imaging and Histopathologic Findings of the Brain in Extremely Sick Preterm Infants

Ursula Felderhoff-Mueser, Mary A. Rutherford, Waney V. Squier, Philip Cox, Elia F. Maalouf, Serena J. Counsell, Graeme M. Bydder, and A. David Edwards

BACKGROUND AND PURPOSE: **MR imaging can now be used safely in extremely preterm infants. The aim of this study was to compare the MR imaging appearance of the immature brain with neuropathologic findings at postmortem examination.**

METHODS: **Seven extremely sick preterm infants, born at a median of 24 weeks' gestation, were studied using T1- and T2-weighted MR sequences. Infants died at a median of 3 days after initial MR imaging, and postmortem examinations were carried out.**

RESULTS: **The cortex and germinal matrix were seen as areas of low signal intensity on T2-weighted images, which corresponded to their highly cellular histologic appearance. The periventricular and subcortical layers of white matter had a high signal intensity, corresponding to high fiber and relatively low cellular density; the intermediate layer of low signal intensity corresponded to a dense band of migrating cells. Regions of acute hemorrhage were seen as low signal intensity and regions of infarction as high signal intensity on T2-weighted images. One infant with mild periventricular leukomalacia had some low signal intensity on T1-weighted images, but no focal changes on T2-weighted images. Regions of neuronal mineralization, seen in association with infarction and capillary proliferation, within the basal ganglia and thalami were characterized by very low signal intensity on T2-weighted images and by very high signal intensity on T1-weighted images. There were no imaging abnormalities detected in regions with more subtle histologic abnormalities, such as increased glial or apoptotic cells.**

CONCLUSION: **MR imaging can be used to observe normal developing brain anatomy in extremely premature infants; it can detect areas of hemorrhage and infarction within the developing brain, but conventional MR imaging may not detect more subtle histologic abnormalities.**

Advances in the understanding of fetal physiology and improvements in neonatal life support have resulted in markedly increased survival rates of very low-birth-weight (<1500 g) infants (1). However, these infants remain at great risk for developing neurologic impairments (2) with a morbidity of up to 68% reported in infants born at or below 25 weeks of gestation (3).

MR imaging provides good anatomic definition of the neonatal brain and therefore has the potential to be of use in following its development and in detecting lesions, which are poorly delineated by sonography. We have installed a unique MR system on our neonatal intensive care unit specifically designed for neonatal use (4, 5). The short bore length of this system provides easy access to the infants during scanning and allows us to study extremely preterm infants while maintaining the same level of intensive care as provided elsewhere in the neonatal unit. As a result, we have been able to image serially preterm infants as immature as 23 weeks' gestational age (6, 7).

Previous correlation between the MR imaging and the histologic appearances of the immature brain has been provided by MR studies performed in utero or postmortem on formalin-fixed brains (8–10). However, the quality of these images is often poor or subject to artifacts.

Received October 29, 1998; accepted after revision April 1, 1999.

U.F-M. was supported by a grant from the Ernst-Schering Foundation, Berlin, Germany. Financial support was also provided by the Garfield Weston Foundation and the United Kingdom Medical Research Council.

From the Department of Pediatrics (U.F-M., M.A.R., E.F.M., A.D.E.), The Robert Steiner Magnetic Resonance Unit (M.A.R., S.J.C., G.M.B.), and the Department of Histopathology (P.C.), Imperial College School of Medicine, Hammersmith Hospital, London; and the Department of Neuropathology, Radcliffe/Infirmary, Oxford (W.V.S.).

Address reprint requests to A. D. Edwards, MD, Department of Paediatrics, Imperial College School of Medicine, Hammersmith Hospital, Du Cane Rd, London W12 ONN, U.K.

Clinical data of premature infants enrolled in this study

Case	Gestational Age (Weeks + Days)			Birth Weight (g)	Clinical Course
	At Birth	At Final MR Study	At Death		
1	26 + 0	29 + 2 (PM)	29 + 2	720	Severe RDS, hypotension, sepsis, bilateral IVH, multisystem failure
2	28 + 0	32 + 0	33 + 0	970	Mild RDS, NEC, sepsis, acute deterioration with hypoxaemia and acidosis on day 30
3	23 + 6	26 + 3	26 + 4	610	Twin pregnancy, severe RDS, hypernatraemia, bilateral IVH, NEC
4	24 + 5	30 + 0 (PM)	30 + 0	640	Triplet pregnancy, RDS, left renal artery stenosis, multiple episodes of sepsis (coagulase neg staph), bilateral IVH, perforated gastric ulcer with peritonitis
5	23 + 6	27 + 4	27 + 4	740	Severe RDS, pneumothorax on day 2, sepsis (candidiasis), NEC
6	26 + 3	29 + 4	29 + 4	800	Antenatal sepsis, RDS, sepsis (*S. aureus*), neurologic problems with severe hypotonia and dystonia, multiple cranial nerve palsies
7	24 + 4	24 + 5		790	Antenatal PV hemorrhages, placental abruption, suspected sepsis

Note.—RDS indicates respiratory distress syndrome; NEC, necrotizing enterocolitis; IVH, intraventricular hemorrhage; PM, postmortem.

The aim of the present study was to compare MR images obtained before or immediately after death with subsequent findings at postmortem neuropathologic examination in order to clarify the histologic correlates of MR signals in these extremely preterm infants.

Methods

Ethical approval for the study of infants with MR imaging was obtained from the Hammersmith Hospitals Research Ethics Committee. Parental consent for imaging the infants and subsequently for postmortem examination of the brain was given in each case. The study group consisted of seven extremely preterm infants admitted to the Hammersmith Hospital neonatal intensive care unit. Gestational age was calculated from the last menstrual period and confirmed with clinical examination and data from early antenatal sonograms.

The infants were born at a median of 24 weeks (range, 23–28 weeks) of gestation with a median birth weight of 740 g (range, 610–970 g). The study group underwent their final MR examinations at a median of 20 days (range, 2–35 days) after birth. At the time of examination all infants were receiving mechanical ventilation. Infants died at a median of 3 days (range, 0–7 days) after MR imaging. Three infants also had a postmortem MR examination on the day of death.

MR Imaging

The 1-T neonatal MR system (Oxford Magnet Technology/Picker International) used in this study has a short bore length of 380 mm, which allows good access to the infant for monitoring and ventilation during scanning (4, 5). For the T1-weighted conventional spin-echo sequences, the parameters were 600/20/2 (TR/TE/excitations); a 4-mm section thickness, with nine sections obtained; and a 192 × 192 matrix. For the T2-weighted fast spin-echo (FSE) sequences, the parameters were 3500/208/2,4; a 4-mm section thickness, with nine sections obtained; an echo train length of 16; interecho spacing of 16; and a 256 × 256 matrix. And for the inversion recovery (IR) FSE sequences, the parameters were 3500/32/4; an inversion time of 950; a section thickness of 5 mm, with six sections obtained; an echo train length of 16; interecho spacing of 16; and a 256 × 256 matrix.

Full intensive care and monitoring were continued throughout the scanning period as described previously (11). All infants were accompanied by at least one experienced pediatrician. Images were reviewed independently by two of the authors who were unaware of the clinical condition of the infants during life, and a final assessment was reached by consensus.

Neuropathologic Examination

Brains were fixed in 10% formalin for a minimum of 5 days prior to examination. The hindbrain was removed by a horizontal cut through the midbrain. The cerebral hemispheres were separated by a sagittal cut through the corpus callosum. After macroscopic assessment, one hemisphere was cut coronally and the other horizontally, corresponding to the MR imaging planes. The cerebellum was cut through the vermis in the sagittal plane, then each hemisphere was cut in an oblique vertical plane through the dentate nucleus. The brain stem was sliced serially, perpendicular to its long axis. After embedding blocks of the entire brain in paraffin wax, 10 μm sections of brain tissue were cut and stained with hematoxylin-eosin or Luxol fast blue/cresyl violet (LB/CV).

Comparisons were made first between the MR images and macroscopic coronal and transverse sections, and then between the corresponding images and microscopic slides.

Results

Clinical information concerning the seven infants in the study is given in the Table.

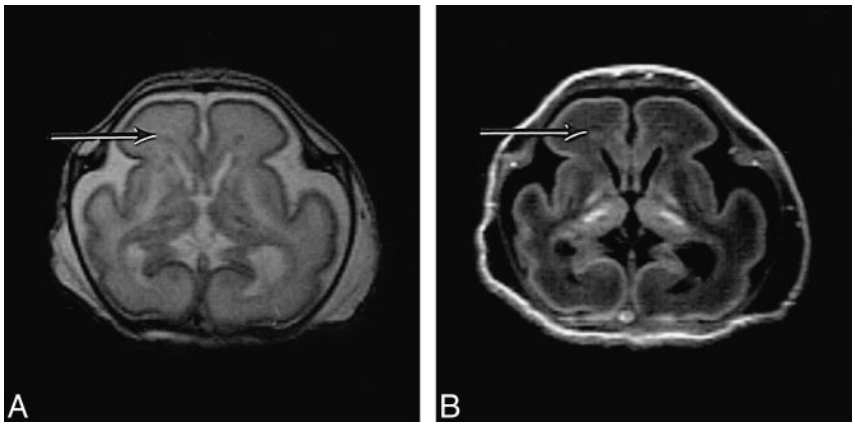

FIG 1. Preterm infant of 26 weeks' (+3 days) gestation (case 6) at age 3 weeks.

A, T2-weighted (3500/208) FSE MR sequence shows the anterior cap within the periventricular white matter as high signal intensity (*arrow*) with a medial low signal component. There are abnormal low signal intensities within the globus pallidus and thalamus.

B, T2-weighted (3500/32/950) IR FSE sequence shows the anterior cap within the periventricular white matter as an area of low signal intensity (*arrow*) with a high-signal medial component. There are abnormal high signal intensities within the globus pallidus, putamen, and thalamus. The posterior limb of the internal capsule is seen as very low signal intensity.

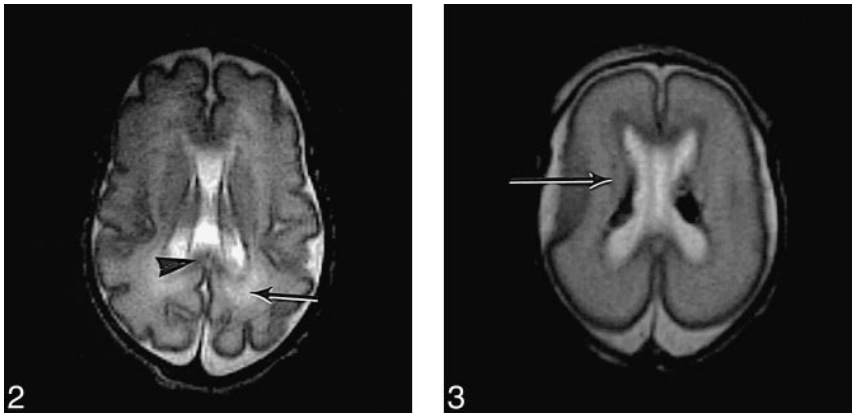

FIG 2. T2-weighted (3500/208) FSE sequence in preterm infant (not in study) of 26 weeks' gestation at age 5 weeks shows normal appearance of the *corpus callosum* (*arrowhead*) in the posterior periventricular white matter (*arrow*).

FIG 3. T2-weighted (3500/208) FSE sequence in preterm infant of 24 weeks' (+4 days) gestation (case 7) at age 2 days shows the intermediate layer of white matter as low signal intensity (*arrow*). There are bilateral low signal intensity germinal layer hemorrhages.

The following imaging results refer to the in vivo MR findings on T2-weighted FSE images, unless otherwise stated. In two infants (cases 1 and 4) the immediate postmortem MR image obtained on the day of death was used for the analysis, as the interval between the final premortem scan and death was 7 days.

Normal Neuroanatomy

None of the infants had completely normal MR findings, but all had regions of the brain that appeared normal on the images.

The previously documented layered appearance of the white matter was demonstrated on MR images (7). For the purposes of this article, we refer to these as periventricular, intermediate, and subcortical layers of the white matter.

Periventricular White Matter.—MR appearance: The periventricular white matter was seen as relatively high (long T2) signal intensity. Around the anterior horn of each ventricle this periventricular layer had the configuration of a cap (Fig 1) and was seen as higher signal intensity than the rest of the periventricular white matter. None of the infants had a region of high (long T2) signal intensity in the shape of an arrowhead around the posterior horn of the lateral ventricle, similar to that which we have described previously (7) (Fig 2).

Histology: The periventricular white matter consisted mainly of fiber bundles, representing the developing white matter, corresponding to the high (long T2) signal intensity on MR images. In the regions seen as higher signal intensity on MR images, the anterior caps, the fibers were more abundant and less organized, with many converging from various directions within the white matter.

Intermediate White Matter.—MR appearance: The intermediate layer was seen as low (short T2) signal intensity (Fig 3). A discrete region of low signal intensity was also seen within the anterior cap (Fig 1).

Histology: The layer of low (short T2) signal intensity corresponded to a cell-rich region. The cells were elongated and arranged longitudinally along radial glia, consistent with the previously described appearance of migrating immature cells. In some areas, particularly frontally, they were also clustered around small radial blood vessels. In the region of the anterior cap, fountains of ''migrating

cells'' were running radially out from the germinal matrix, corresponding to the discrete region of low (short T2) signal intensity on MR images.

Subcortical White Matter.—MR appearance: The subcortical layer of white matter was seen as relatively high (long T2) signal intensity.

Histology: The subcortical white matter consisted mainly of radial fibers with relatively few cells.

The Cortex.—MR appearance: The cortex appeared as a ribbon of low (short T2) signal intensity. It was not possible to differentiate the layers of the cortex with MR imaging in any infant.

Histology: The cortex was densely cellular with short processes on some cells. There was partial lamination of layers I and II in the two infants younger than 27 weeks' gestation and partial lamination of all cortical layers in the remaining five infants, who were all older than 27 weeks' gestation.

Corpus Callosum.—MR appearance: The corpus callosum was clearly visible as a thin region of low (short T2) signal intensity (Fig 2), anterior and posterior to the lateral ventricles on transverse images.

Histology: The corpus callosum consisted of very tightly packed parallel fibers with very little myelin on LB/CV staining.

Basal Ganglia and Thalamus.—MR appearance: The basal ganglia appeared as an area of diffuse low (short T2) signal intensity. The region of the ventrolateral nuclei of the thalami had even lower signal intensity within the thalami.

Histology: The basal ganglia and thalamus had a high cellular density as compared with the white matter. The ventrolateral nuclei were well circumscribed and had a higher cellular density than the surrounding thalamic tissue. More generalized differences in cellular density within the basal ganglia and thalami were identified at histology but not appreciated on MR images.

The Internal Capsule.—MR appearance: The position of the posterior limb of the internal capsule was detected as a line of high (long T2) signal intensity. The anterior limb was isointense.

Histology: The orientation of fibers within the internal capsule was noted to be different in the anterior and posterior limbs. On transverse sections through the brain, the fibers in the anterior limb were running in the transverse plane and those in the posterior limb were running at right angles to this plane. Some myelin was identified with LB/CV staining within the posterior limb and, to a lesser extent, within the anterior limb. There were few cells present within the internal capsule.

Hippocampus.—MR appearance: The hippocampal region was noted to have a diffuse low (short T2) signal intensity. Obtaining a clear definition of the component parts of the medial temporal lobe was difficult.

Histology: The hippocampus, which develops by in-folding of the cortex, was seen as a region with high cellular density, corresponding to the low signal intensity on MR images.

Brain Stem.—MR appearance: The signal intensity of the brain stem appeared isointense with that of white matter on T2- and T1-weighted images. The posterior part, with the inferior colliculi and the lateral lemnisci, was visible as a region of low signal on T2-weighted images, consistent with myelination.

Histology: The brain stem, with cell-rich nuclei and fiber bundles, had a normal histologic appearance. Specific myelin staining was not used.

Cerebellum.—MR appearance: The cerebellar cortex was visible as a line of low signal intensity, and the parenchyma consisted mainly of high signal intensity. The inferior cerebral peduncles were seen as areas of low signal intensity on T2-weighted images, consistent with myelination.

Histology: The low (short T2) signal intensity cortex corresponded to areas with high cellular density. Areas of white matter with relatively high signal intensity corresponded to regions with low cellular density and high fiber density. All infants had some abnormal histologic findings. Specific myelin staining was not used.

Germinal Matrix.—MR appearance: The germinal matrix was seen as an extensive region of low (short T2) signal intensity that lined the lateral ventricles on T2-weighted FSE images (high signal intensity on T1-weighted images). The ependymal lining could not be identified separately on MR images.

Histology: The low (short T2) signal intensity matrix corresponded to a region of densely packed immature cells; the innermost layer of the matrix was lined by ependyma.

Abnormal Findings

Intraventricular and Germinal Matrix Hemorrhage.—MR appearance: Bilateral intraventricular hemorrhage with involvement of the germinal layer was detected in five patients (case 1, 3, 4, 5, and 7). In three infants this had a low signal intensity on T2-weighted FSE images (Fig 3) and high signal intensity on T1-weighted images, consistent with recent hemorrhage. In two infants (cases 1 and 5) there was some additional high signal intensity within the germinal layer on T2-weighted images, consistent with older hemorrhage. Hemorrhage was differentiated from the normal germinal matrix by its site and shape. In two infants (cases 1 and 3) the germinal layer hemorrhage extended into the head of the caudate nucleus.

Histology: The presence of both intraventricular and germinal layer hemorrhages was confirmed on macroscopic examination of the brain in all infants. In cases 1, 5, and 7, brown staining of the macrophages laden with red blood cells was noted, suggesting hemorrhage of at least 1 week. Involvement of the head of the caudate nuclei in cases 1 and 3 was confirmed at histology.

Parenchymal Venous Infarction.—MR appearance: In two patients (case 1 and 3), MR images

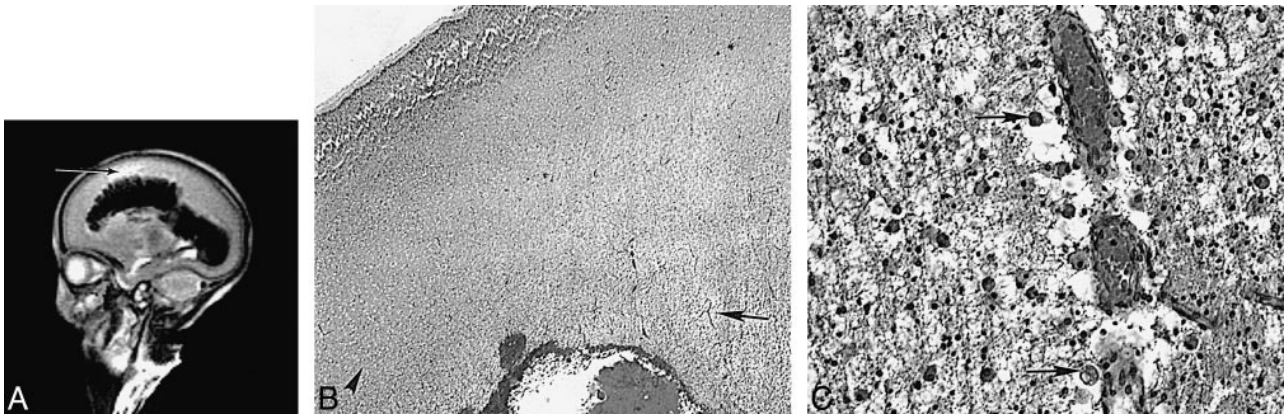

FIG 4. Preterm infant of 23 weeks' (+6 days) gestation (case 3) at age 3 weeks.

A, T2-weighted (3500/208) FSE sequence shows a large intraventricular hemorrhage with fan-shaped parenchymal involvement. The perihemorrhagic white matter is of very high signal intensity (*arrow*).

B, Histologic section shows intraventricular hemorrhage. A zone of venous infarction radiates out into the white matter from the site of bleeding (*arrow* in center of infarct). Relatively normal white matter is seen to the left of the picture (*arrowhead*). The infarcted area is very pale owing to tissue loss (hematoxylin-eosin, original magnification ×22.5).

C, Higher-magnification histologic section of the venous infarction shows very congested capillaries. The adjacent tissue contains many large macrophages with ingested red cells (*arrows*). There are few free red cells. The tissue shows early cystic breakdown (hematoxylin-eosin, original magnification ×360).

showed a fan-shaped area of low signal intensity on T2-weighted FSE sequences with linear projections radiating out from the ventricular wall into the white matter (Fig 4A), following the distribution of the medullary veins (12). The white matter around these fan-shaped areas had abnormally high signal intensity on T2-weighted images.

Histology: The fan-shaped structure of low signal intensity corresponded to edematous white matter containing congested radial blood vessels cuffed by macrophages containing red blood cells (Fig 4B and C). There were few free red blood cells within the parenchyma, but large numbers of macrophages with phagocytosed red cells were seen. These changes, consistent with venous infarction, formed a well-defined wedge extending from the site of the hemorrhage in the germinal matrix out to the cortex. Adjacent white matter, with abnormal high signal intensity on MR images, showed edema and axon retraction balls, consistent with infarction.

White matter.—MR appearance: Two infants (cases 1 and 3) had regions of venous infarction, as already described. Two infants (cases 6 and 7) had a relatively normal appearance of the white matter on imaging, although posterior arrowheads were not visible within the periventricular white matter. The remaining three infants (cases 2, 4, and 5) showed some disruption of the normal banded appearance of the white matter with loss of the anterior caps. One of these infants (case 2) showed generally low signal intensity throughout, with multiple punctate areas of even lower signal posteriorly on T1-weighted images. The second infant (case 4) showed patchy alterations of both high and low signal intensity with both T1- and T2-weighted sequences, which were most marked in the periventricular white matter (Fig 5). The third infant (case 5) had small areas of increased signal intensity in the periventricular white matter on T1-weighted sequences.

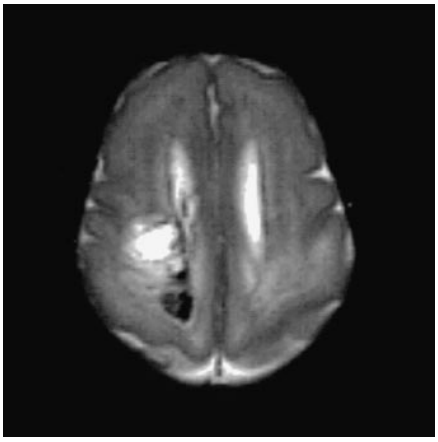

FIG 5. Postmortem T2-weighted (3500/208) FSE sequence in preterm infant of 2 weeks' (+5 days) gestation (case 4) shows bilateral abnormal signal intensity within the posterior periventricular white matter and a low signal intensity hemorrhagic component on the right.

Histology: One of the two infants with near normal imaging appearances of the white matter had normal histologic findings, but the second infant (case 7) had numerous microglial cells and apoptotic cells, consistent with diffuse injury. Of the three infants (cases 2, 4, and 5) who had more marked loss of the normal white matter architecture on MR images, case 2 had gliosis, increased capillary density, and some focal mineralization, consistent with periventricular leukomalacia; case 5 had edema and pyknotic cells, congested capillaries, and numerous well-circumscribed lesions secondary to candidiasis, with no lines of migrating cells in the region of the anterior cap; and case 4 had pyknotic cells and axon retraction balls in the

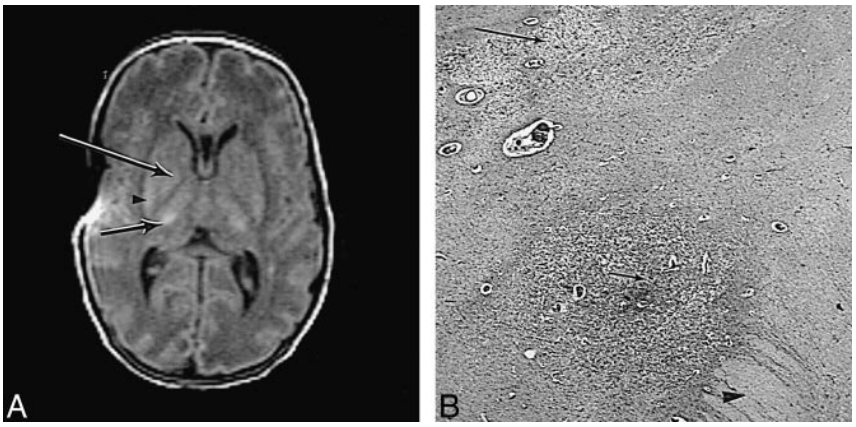

FIG 6. Preterm infant of 28 weeks' gestation (case 2) at age 4 weeks.

A, T1-weighted (600/20) SE sequence shows abnormal high signal intensity within the posterior putamen (*arrowhead*), globus pallidus (*long arrow*) on the right, and lateral thalamus (*short arrow*). The posterior limb of the internal capsule is of uniform low signal intensity. There is an artifact of uncertain origin over the right insula cortex.

B, High-power histologic section of damaged deep gray matter shows that the posterior limb of the internal capsule is edematous (*arrowhead*). The adjacent globus pallidus is darkly stained owing to capillary proliferation and mineralization of dead neurons (*short arrow*). The posterior part of the putamen is pale as a result of extensive tissue loss (*long arrow*) (hematoxylin-eosin, original magnification × 22.5).

periventricular white matter, consistent with recent infarction, and there was fresh hemorrhage, presumed to be a terminal event, with reactive microglial cells in the subcortical white matter.

Basal Ganglia and Thalami.—MR appearance: Marked abnormalities within the basal ganglia and thalami were noted in two infants (cases 2 and 6). These were of very low signal intensity on T2-weighted images and of very high signal intensity on T1-weighted images within the globus pallidus and thalamus (Figs 1 and 6). These infants had abnormal regions of high signal intensity within the posterior putamen on T1-weighted spin-echo sequences but no areas of low signal intensity on T2-weighted images. In the remaining five infants, the MR appearance was normal.

Histology: The combination of very low signal intensity on T2-weighted images and very high signal intensity on T1-weighted images corresponded particularly to the presence of clusters of mineralized neurons within areas of established infarction with capillary proliferation. Vacuolation was also seen. Within the putamen there was edema with increased glial cells, apoptotic cells, and capillary proliferation. Vacuolation was particularly prominent, but there were no mineralized neurons (Fig 6B). The five remaining infants with normal MR appearances of the basal ganglia and thalami had histologic abnormalities that were not associated with obvious abnormal signal intensities on MR images. Three infants had increased numbers of apoptotic cells within the caudate head, and all three had germinal layer hemorrhage overlying the caudate head on MR images. Two infants had apoptosis in the putamen and necrotic cells in the globus pallidus.

Posterior Limb of the Internal Capsule.—MR appearance: There was an exaggeration of the normal high (long T2) signal intensity in the posterior limb of the internal capsule in three infants (cases 2, 3, and 6) (Figs 1 and 6). The signal intensity was normal in the remaining four infants.

Histology: There was marked edema within the posterior limb in all three infants, corresponding to the abnormally high signal intensity on MR images (Fig 6B). There was no edema in the remaining four infants in whom signal intensity was normal.

Hippocampus.—MR appearance: In six infants, the MR appearance was apparently normal. Abnormalities in the hippocampus were only detected on MR images in one infant (case 5) who had some loss of the normal high signal intensity on T1-weighted spin-echo images.

Histology: Two infants with normal MR appearances had normal histologic findings. The remaining four infants who had normal MR appearances had abnormal histologic findings: neuronal necrosis in two, focal neuronal loss in one, and increased microglial cells in one. One infant had abnormal MR appearances and at histology there were some small areas of necrosis consistent with foci of *Candida albicans* and an increase in pyknotic cells, as described previously.

Brain Stem.—MR appearance: Two infants (cases 2 and 6) had abnormalities with excessively high signal intensity on T2-weighted images (low on T1-weighted images). Imaging was unremarkable in the remaining five infants.

Histology: There was extensive bilateral symmetrical infarction of the tegmental region in both infants in whom abnormal high signal intensity was seen. The remaining five infants had less marked abnormalities at histology, with small areas of necrosis or increased glial cells. Myelin staining was not performed.

Cerebellum.—MR appearance: There were no obvious abnormalities in the cerebellum on MR im-

ages; however, visualization of the cerebellum in many of the images was suboptimal.

Histology: Despite the normal MR appearance, specimens from all infants showed abnormalities on histologic examination. Two infants had severe abnormalities consistent with infarction (cases 2 and 6), the remaining infants had more subtle abnormalities, including neuronal necrosis in three, focal neuronal loss in one, and increased glial cells in one. Myelin staining was not performed.

Discussion

Imaging of preterm infants has been limited in the past because MR systems were primarily designed for adult imaging, making it difficult to access infants and to provide continuous intensive care.

In this study, a unique MR system, designed for neonatal investigations, was used to delineate the structure of the brain and to describe pathologic changes in extremely preterm infants, ranging from 24 to 32 weeks' gestation. The MR appearances were then compared with findings at postmortem examination.

Our study group comprised a small number of infants who had both early MR imaging and neuropathologic postmortem examination. Prior to death, many infants were too sick to image and therefore the gap between MR examination and death was sometimes several days. In two infants (cases 1 and 4), the gap was 7 days, and therefore an immediate postmortem image was performed and used for comparison.

Because none of the remaining infants was imaged on the day of death, and because pathologic lesions may have occurred after the last image and before or during death, it is likely that we have underestimated the ability of MR imaging to detect abnormalities within the immature brain. In addition, lesions take time to evolve, both at imaging and on histology, so there may be little change early after an insult. Diffusion-weighted imaging may have been able to detect more subtle or early abnormalities, but we were unable to include this sequence in our imaging protocol.

The results showed a clear relationship between the MR signal intensity and the cellular density of the developing brain and documented the MR appearance of histologically normal areas of the developing brain. Regions that were noted to be highly cellular at histology, the germinal layer, the cortex, and the migrating cell layer, were seen as regions of low signal intensity on T2-weighted images. The migrating cells were seen most clearly in the vicinity of the anterior cap, where cells were aligned on radial fibers spreading out from the cap allowing the cells to line up in ''fountains.'' For regions that consisted mainly of white matter fibers, the periventricular and subcortical white matter was seen as high signal intensity on T2-weighted images. Within the periventricular white matter the anterior caps were seen as even higher signal intensity. On histologic examination, these caps consisted of bundles of fibers converging from several directions. We did not see the corresponding posterior arrowheads within the periventricular white matter in any of the infants. Their absence may in part be due to extreme immaturity but may be associated with the relatively subtle pathologic changes that we detected at histology.

The relationship between signal intensity and cellular density has been reported previously (8, 9). A recent article described the presence of multiple low signal intensity bands in the white matter of some very premature infants (13). These authors postulated that these multiple bands represented migrating glial cells. We were not able to detect multiple bands either at MR imaging or histology in the infants in our study. The number of apparent bands identified may depend on image resolution, although motion artifacts and partial volume effects from the insular cortex may give similar appearances.

The signal intensity of white matter tracts may be influenced by the orientation of fibers as well as by their density. The different signal intensities noted within the anterior and posterior limb of the internal capsule may be attributable to different orientation of their constituent fibers. Although the corpus callosum contains many fibers and has a very low cellular density, it had low signal intensity, similar to that in the cortex. This low signal intensity was not explained by the presence of myelin, although only LB/CV staining was used and the amount of myelin present may have been underestimated. One explanation may be that the fibers of the corpus callosum were very closely packed, which may have decreased the regional water content and thereby decreased the TI and T2 of the structure.

The signal intensity of the germinal layer hemorrhage was consistent with the age of the hemorrhage as detected at regular cranial sonography. In the older hemorrhages, the regions of short T1 became less obvious and regions of long T2 were seen within the short T2 areas, reflecting the presence of the extracellular methemoglobin component of a late subacute hemorrhage. In case 7, the finding of brown staining of the macrophages at histology following death on day 5 suggests an antenatal onset of the hemorrhage.

While MR imaging is very sensitive to the presence of hemorrhage, the MR appearance of an acute hemorrhagic venous infarct in a preterm infant has only recently been described (14). The appearance of a wedge-shaped density radiating out from a germinal-layer hemorrhage has been described previously on sonograms (15). The alterations in MR signal found in this study were consistent with the histologic finding of congested medullary veins and perivascular hemorrhage. The white matter surrounding these hemorrhagic lesions showed abnormally high signal intensity on T2-

weighted images, consistent with edema or infarction; the latter was confirmed at histology.

The MR changes associated with the histologic appearance of focal periventricular leukomalacia were relatively subtle and were not associated with cystic lesions on sonograms at the time of MR imaging. One infant (case 7) with histologic changes consistent with a more diffuse but less severe white matter injury had normal MR findings, although the posterior arrowheads were not seen. The cellular changes were similar to those found in the infant with focal periventricular leukomalacia but were more diffuse and not associated with discrete infarcts. These appearances have been described as diffuse periventricular leukomalacia (16) and may also be consistent with the white matter changes of perinatal teloleukoencephalopathy described by several authors (17, 18). An association between perinatal teloleukoencephalopathy and endotoxemia has been described (19). In case 7 of this study there were several episodes of vaginal bleeding during the pregnancy, and perinatal sepsis was suspected but not proved after delivery.

We were able to identify severe ischemic lesions in the basal ganglia and thalami with MR imaging. Lesions in the basal ganglia and thalami are usually associated with hypoxic-ischemic injury in the term brain. However, the lesions are associated with a severe acute hypoxic-ischemic insult, which may occur at any gestational age, but occurs more frequently in the term infant (20). The two study infants with these lesions had a history of a severely acute hypoxic-ischemic event. In both infants the presence of neuronal mineralization was associated with well-defined regions of very short T1 and short T2 (Figs 1 and 6) and was seen in the globus pallidus and thalamus, but not within the striatum. The different pathologic changes within the basal ganglia and thalami may in part be related to their inherently different cellular densities. We did not look specifically at the type of mineralization (21). There were no clear signal intensity changes associated with the finding of increased apoptosis in the caudate head, again reflecting the inability of conventional MR imaging to identify areas with more subtle pathologic changes.

Localization of lesions was more difficult in smaller brain structures, such as the brain stem, the hippocampus, and the cerebellum. Visualization of these structures is often suboptimal owing to artifacts or levels and angles of acquisition of the images. Major abnormalities, such as necrosis and infarction, were detected on MR images in the brain stem and the hippocampus but not in the cerebellum. The lack of MR findings in the cerebellum has also been reported in studies of severely asphyxiated preterm infants and in the asphyxiated term infant (21, 22).

Imaging studies of ex-preterm infants have reported a high prevalence of abnormalities consistent with aberrant white matter development, such as ventricular dilatation, poor myelination, and increased gliotic tissue (23). In a cohort of surviving preterm infants without major brain lesions we have documented a high rate of occurrence of patchy hyperintense regions of white matter on T2-weighted FSE images. These regions develop after 30 weeks' gestation and, at term-equivalent age, are associated with the development of ventricular dilatation and some atrophy of the brain (24). It is possible that these late imaging changes arise from small areas of periventricular leukomalacia, as we have described, and/or from diffuse white matter injury. This cohort cannot be directly compared with the very sick infants in this small study, none of whom had the typical white matter hyperintense changes prior to death.

Conclusion

While conventional MR imaging accurately identified normal anatomic structures and regions of infarction and hemorrhage, it was not able to detect more subtle histologic abnormalities, such as increased glial cells or increased apoptosis. More sophisticated imaging techniques, such as diffusion-weighted imaging or MR spectroscopy, may prove to be more sensitive to these more subtle abnormalities. Long-term prospective studies may enable us to establish early imaging correlates for many more of the neurologic impairments identified in children who have been born prematurely.

Acknowledgments

We thank the members of the neonatal intensive care unit of Hammersmith Hospital for their assistance.

References

1. Tin W, Wariyar U, Hey E. **Changing prognosis for babies of less than 28 weeks gestation in the north of England between 1983 and 1994: Northern Neonatal Network.** *BMJ* 1997;314:107–111
2. Horwood LJ, Mogridge N, Darlow BA. **Cognitive, educational and behavioural outcomes at 7 to 8 years in a national very low birthweight cohort.** *Arch Dis Child Fetal Neonatal Ed* 1998; 79:F12–F20
3. Emslie HC, Wardle SP, Sims DG, Chiswick ML, D'Souza SW. **Increased survival and deteriorating developmental outcome in 23–25 weeks gestation infants: 1990–1994 compared with 1984–1989.** *Arch Dis Child Fetal Neonatal Ed* 1998;78:99–104
4. Hall AS, Young IR, Davies FJ, Mohaparta SN. **A dedicated magnetic resonance system in a neonatal intensive therapy unit.** In: Bradley WG, Bydder GM, eds. *Advanced MR Imaging Techniques.* London: Martin Dunitz; 1997:281–289
5. Maalouf E, Counsell S, Battin M, Cowan F. **Magnetic resonance imaging of the neonatal brain.** *Hosp Med* 1998;59:41–45
6. Battin MR, Maalouf EF, Counsell SJ, Herilhy AH, Edwards AD. **Magnetic resonance imaging of the brain of premature infants.** *Lancet* 1997;349:–1741
7. Battin MR, Maalouf EF, Counsell SJ, et al. **Magnetic resonance imaging of the brain in very preterm infants: visualization of the germinal matrix, early myelination and cortical folding.** *Pediatrics* 1998;101:957–962
8. Brisse H, Fallet C, Sebag G, Nessmann C, Blot P, Hassan M. **Supratentorial parenchyma in the developing fetal brain: in vitro MR study with histologic comparison.** *AJNR Am J Neuroradiol* 1997;18:1491–1497
9. Girard N, Raybaud C, Poncet M. **In vivo MR study of brain maturation in normal fetuses.** *AJNR Am J Neuroradiol* 1995; 407–413

10. Sibony O, Stempfle N, Luton D, Oury JF, Blot PH. **In utero fetal cerebral intraparenchymal ischemia diagnosed by nuclear magnetic resonance.** *Dev Med Child Neurol* 1998;40:122–123
11. Battin MR, Maalouf EF, Counsell SJ, et al. **Physiological stability of preterm infants during magnetic resonance imaging.** *Early Hum Dev* 1998;58:101–110
12. Gould SJ, Howard S, Hope PL, Reynolds OR. **Periventricular intraparenchymal cerebral hemorrhage in preterm infants: the role of venous infarction.** *J Pathol* 1987;151:197–202
13. Childs A-M, Ramenghi LA, Evans DJ, et al. **MR features of developing periventricular white matter in preterm infants: evidence of glial cell migration.** *AJNR Am J Neuroradiol* 1998; 19:971–976
14. Counsell S, Maalouf EF, Rutherford MA, Edwards AD. **Periventricular haemorrhagic infarct in a preterm neonate.** *Eur J Pediatr Neurol* 1999;3:25–28
15. Hope P, Gould SJ, Howard S, Hamilton PA, Costello AM, Reynolds EO. **Precision of ultrasound diagnosis of pathologically verified lesions in the brains of very preterm infants.** *Dev Med Child Neurol* 1988;30:457–471
16. Volpe J. ***Neurology of the Newborn.*** 3rd ed. Philadelphia: Saunders; 1995
17. Leviton A, Gilles FH. **An epidemiologic study of perinatal leucoencephalopathy in an autopsy population.** *Am J Epidemiol* 1976;104:621–626
18. Paneth N, Rudelli R, Monte W, et al. **White matter necrosis in very low birth weight infants: neuropathologic and ultrasonographic findings in infants surviving six days or longer.** *J Pediatr* 1990;116:975–984
19. Gilles FH, Averill DR Jr, Kerr CS. **Neonatal endotoxin encephalopathy.** *Ann Neurol* 1977;2:49–56
20. Barkovich AJ, Sargent SK. **Profound asphyxia in the premature infant: imaging findings.** *AJNR Am J Neuroradiol* 1995;16:1837–1846
21. Barkovich AJ, Truwit LT. **Brain damage from perinatal asphyxia: correlation of MR findings with gestational age.** *AJNR Am J Neuroradiol* 1990;11:1087–1096
22. Rutherford M, Pennock J, Schwieso J, Cowan F, Dubowitz L. **Hypoxic-ischaemic encephalopathy: early and late magnetic resonance imaging findings in relation to outcome.** *Arch Dis Child Fetal Neonatal Ed* 1996;75:145–151
23. Skranes JS, Nilsen G, Smevik O, Vik T, Brubakk AM. **Cerebral MRI of very low birthweight children at 6 years of age compared with the findings at 1 year.** *Pediatr Radiol* 1998;28:471–475
24. Maalouf EF, Duggan P, Rutherford, et al. **MRI of the brain in extremely preterm infants: normal and abnormal findings from birth to term.** *J Pediatr* (in press)